

Incommensurate spin-density-wave order in quasi-one-dimensional metallic antiferromagnet NaV_2O_4

Hiroshi Nozaki,^{1,*} Jun Sugiyama,¹ Martin Månsson,² Masashi Harada,¹ Vladimir Pomjakushin,² Vadim Sikolenko,² Antonio Cervellino,³ Bertrand Roessli,² and Hiroya Sakurai⁴

¹Toyota Central Research and Development Laboratories Inc., Nagakute, Aichi 480-1192, Japan

²Laboratory for Neutron Scattering, ETH Zürich and Paul Scherrer Institut, CH-5232 Villigen PSI, Switzerland

³Swiss Light Source, Paul Scherrer Institut, CH-5232 Villigen PSI, Switzerland

⁴National Institute for Materials Science, Namiki, Tsukuba, Ibaraki 305-0044, Japan

(Received 24 February 2010; published 23 March 2010)

To clarify the reason for the coexistence of long-range antiferromagnetic order and metallic conductivity for NaV_2O_4 , in which the V ions form quasi-one-dimensional zigzag chains along the b axis, we have performed a neutron-scattering experiment using a powder sample down to 20 K. The analysis of the magnetic powder diffractogram below $T_N=140$ K demonstrates the formation of an incommensurate spin-density-wave order with $\mathbf{k}=(0,0.191,0)$; the ordered moment was estimated as $(0,0,0.77\mu_B)$ at 20 K.

DOI: 10.1103/PhysRevB.81.100410

PACS number(s): 75.30.Fv, 75.25.-j

Itinerant antiferromagnetism (AF) in general, and for quasi-one-dimensional systems, in particular, remains one of the big unresolved problems in condensed-matter physics. Since conduction electrons are naturally hindered in their cooperative motion by the spin order,¹⁻³ the main issue is to clarify how metallic conductivity and AF order can coincide. In order to solve this puzzle, the AF spin structure is thus expected to be unconventional compared to those for insulating AF compounds.

The title compound is a very recent arrival among the metallic AF systems because NaV_2O_4 is only obtained by a high-pressure synthesis technique.⁴ NaV_2O_4 belongs to the CaFe_2O_4 -type orthorhombic structure with space group $Pnma$. Here, V_2O_4 double-leg chains, i.e., zigzag chains formed by a network of edge-sharing VO_6 octahedra align along the b axis so as to make an irregular hexagonal one-dimensional (1D) channel (see Fig. 1). Because of a mixed-valence state of the V ions (+3.5), NaV_2O_4 exhibits metallic conductivity down to 40 mK while susceptibility (χ) measurements indicate an AF transition with $T_N=140$ K.⁴ Magnetic anisotropy measurements using single-crystal samples suggested that the intraleg interaction is ferromagnetic (FM) while the interleg interaction is AF, i.e., nearest-neighbor J_1 is positive and next-nearest-neighbor J_2 is negative.

Although theoretical treatments of the zigzag chain compounds with $S=1/2$ and $S=1$ are available,⁵⁻⁸ there are, to the authors' knowledge, very limited investigations regarding the ground state of a mixed-valence state.^{9,10} Recent positive muon-spin-relaxation/rotation ($\mu^+\text{SR}$) measurements¹¹ clarified the existence of static AF order below T_N and suggested a complex magnetic ground state based on the observation of oscillatory signals in zero applied field (ZF). That is, the ZF- $\mu^+\text{SR}$ spectrum consisted of mainly four signals below 120 K and one signal above 120 K (and up to T_N), implying the existence of one more transition at 120 K ($=T_{N2}$). The delay of the initial phase of the cosine function for fitting a ZF spectrum below T_N should be (close to) zero for a simple commensurate spin structure.¹² In the NaV_2O_4 case, nonzero initial phases indicated a complex ground state. However, since $\mu^+\text{SR}$ does not provide information on the correlation

length of magnetic order,¹² it is very difficult to determine the AF spin structure solely by $\mu^+\text{SR}$. On the other hand, for long-range magnetic order, neutron scattering is a direct method to detect magnetic order as magnetic Bragg peaks. In this Rapid Communication we present data from neutron-diffraction measurements on NaV_2O_4 . Together with synchrotron-radiation x-ray diffraction (SR-XRD) and previous $\mu^+\text{SR}$ data, we demonstrate the formation of an incommensurate spin-density-wave (IC-SDW) order below $T_N=140$ K.

A polycrystalline sample of NaV_2O_4 was prepared by a solid-state reaction technique under a pressure of 6 GPa using $\text{Na}_4\text{V}_2\text{O}_7$ and V_2O_3 powders as starting materials. A mixture of the two powders was packed in an Au capsule, then heated at 1300 °C for 1 h, and finally quenched to ambient T . A powder XRD analysis showed that the samples were single phase with an orthorhombic system of space group $Pnma$ at ambient T . DC- $\chi(T)$ data from the present sample reproduce the prior measurements reported in Ref. 13. The preparation and characterization of the samples were described in greater detail elsewhere.¹³ Neutron-scattering experiments were performed in the T range between 20 and 150 K, using the HRPT (Ref. 14) to get high resolution powder diffraction data as well as DMC (Ref. 15) station to detect the magnetic diffraction peaks of SINQ at the Paul Scherrer Institute (PSI), Switzerland. The SR-XRD measurements were performed using the X04SA beamline¹⁶ of SLS

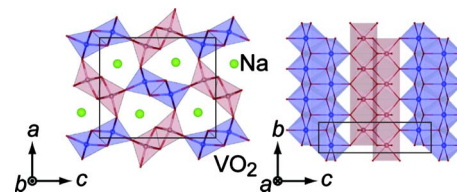


FIG. 1. (Color online) Crystal structure of NaV_2O_4 . The V_2O_4 double chains, i.e., zigzag chains are formed by a network of edge-sharing VO_6 octahedra align along the b axis so as to make an irregular hexagonal 1D channel. The Na ions are located in the center of the 1D channel.

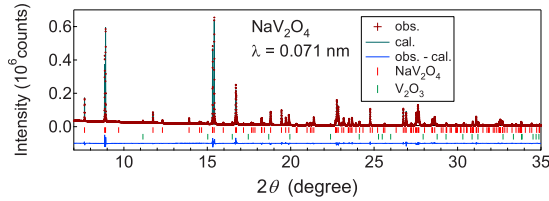


FIG. 2. (Color online) SR-XRD pattern at $T=150$ K and fit result by Rietveld analysis where the reliability (R) factor was minimized down to 4.96%. The diffraction peaks from the V_2O_3 phase are also observed. However, since its mass fraction is estimated as 1.3%, the V_2O_3 phase is eventually ignorable for the present structural and magnetic-structural analyses.

at PSI. The diffraction data were analyzed using both FULLPROF (Ref. 17) and RIETAN-2000.¹⁸

Prior to the neutron experiment, we investigated the existence/absence of structural changes at T_N . Figure 2 shows the XRD and Rietveld refinement pattern for the SR-XRD data acquired at 150 K. We obtained a reliable fit by Rietveld analysis using the space group of $Pnma$ with $a=0.9173(2)$ nm, $b=0.28909(4)$ nm, and $c=1.0682(2)$ nm. Further, XRD patterns were acquired as a function of $T=70$ –300 K and fitted using the same space group. Figure 3 shows the T dependencies of the lattice parameters, i.e., a , b , and c , and the unit-cell volume (V). As T decreases from 300 K, all the parameters show a monotonic change down to 120 K. This clearly excludes a structural transition at T_N .

Figure 4(a) shows the neutron powder-diffraction (NPD) patterns measured at 20 and 150 K. At 20 K, i.e., well below $T_N=140$ K, several magnetic Bragg peaks are clearly seen and they are indexed with the propagation vector $\mathbf{k}=(q_x, q_y, q_z)=(0, 0.191, 0)$. This means that the AF structure is IC to the lattice period along the b axis. As T increases from 20 K, the square-root intensity of the $0\ q_y\ 0$ peak (I_{0q_y0}) decreases and finally disappears at 140 K ($=T_N$) [see Fig. 4(c)], as expected for the order parameter of the AF transition. This is very consistent with the prior μ^+ SR results.¹¹ The $I_{0q_y0}(T)$ curve (and the μ^+ SR data) is well explained by the BCS prediction¹⁹ for an order parameter of the SDW state [see Fig. 4(c)]. Further, it was difficult to fit the data by a mean-field theory, i.e., $I/I_{T=0\text{ K}}=[(T_N-T)/T_N]^\beta$,

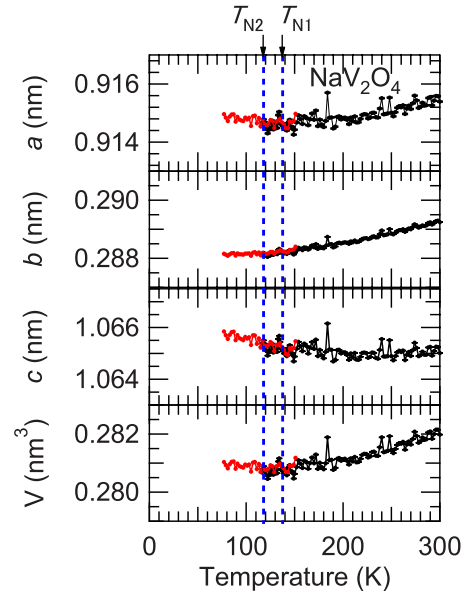


FIG. 3. (Color online) T dependences of lattice parameters and unit-cell volume for NaV_2O_4 obtained by Rietveld analysis. Gray (red online) and black symbols denotes the data taken using He-flow cryostat and liquid N_2 cryojet, respectively.

which implies the formation of a IC-SDW order below T_N , as in the case of, e.g., the organic compound $(\text{TMTSF})_2\text{PF}_6$.²⁰

We extracted eight possible models that agreed with both the crystal symmetry and the propagation vector \mathbf{k} , $\Gamma_{i,S}$ and $\Gamma_{i,H}$ with $i=1-4$ (where S means SDW order and H means helical order). We found that $\Gamma_{3,S}$ (with SDW order) provided the best fit to the experimental data [see Table I and Fig. 4(b)]. That is, the magnetic moment \mathbf{m}_l at the l th V site is represented by

$$\mathbf{m}_l = \mathbf{m}_0 \cos(2\pi \mathbf{k} \cdot \mathbf{l}), \quad (1)$$

where $\mathbf{m}_0=(0, 0, 0.77\mu_B)$ at 20 K. In other words, the V moments align parallel/antiparallel to the c axis but their amplitude is modulated along the b axis with the period of $(\sim 1/0.191=5.26) \times b$ (see Fig. 5). It is thus found that the interleg interaction is FM and the intraleg interaction is AF,

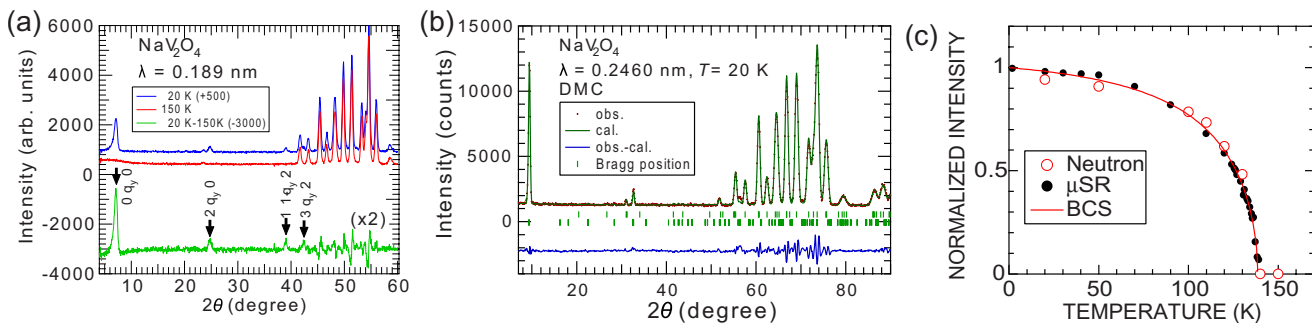


FIG. 4. (Color online) (a) NPD patterns obtained at 20 and 150 K, and their difference. At least, four magnetic Bragg peaks are clearly observed and they are indexed by an incommensurate propagation vector with $\mathbf{k}=(0, 0.191, 0)$. (b) Fit result for the NPD pattern obtained at 20 K using a SDW model along the b axis ($\Gamma_{3,S}$). (c) T dependence of the normalized square root of the intensity of the magnetic Bragg peak $0\ q_y\ 0$. The μ^+ SR result (muon-spin precession frequency f_μ in ZF) is also plotted for comparison; below 120 K, the second highest f_μ among the four f_μ 's is plotted, as it is continuous to f_μ above 120 K. The solid line in (c) represents the T dependence of the BCS gap energy.

TABLE I. Bragg- and magnetic- R factors (R_B and R_m) for the eight possible Γ models for the Neutron data. The fit using $\Gamma_{3,S}$ yields the lowest R_B and R_m (shown in bold) among them. The fit was performed by the program FULLPROF (Ref. 17).

Model	R_B	R_m
$\Gamma_{1,S}$	2.75	39.98
$\Gamma_{2,S}$	2.33	19.19
$\Gamma_{3,S}$	1.79	10.76
$\Gamma_{4,S}$	1.80	17.47
$\Gamma_{1,H}$	2.79	90.60
$\Gamma_{2,H}$	2.33	17.78
$\Gamma_{3,H}$	2.43	39.25
$\Gamma_{4,H}$	2.51	82.93

contrary to prediction from magnetization measurements of single-crystal samples.⁴ Such prediction was, however, solely based on the typical AF behavior in the $\chi(T)$ curve at T_N , the positive paramagnetic Curie temperature ($\Theta_p=118$ K), and the absence of a FM loop in the $M(H)$ curve obtained with both $H\parallel b$ and $H\perp b$, together with the metallic conductivity along the b axis. Note that the $\Gamma_{3,S}$ magnetic structure is against to the magnetic anisotropy of the single crystal measured at $H=50$ kOe.⁴ However, the easy magnetization axis of the low-dimensional system is known to change with applied H .²¹ Thus, although the magnetic anisotropy was reported only at $H=50$ kOe for NaV_2O_4 , it is speculated that the easy magnetization axis is not the b axis but the c axis at low H and/or ZF. This is a reasonable explanation both for the proposed SDW structure and magnetic anisotropy of NaV_2O_4 .

From a recent μ^+ SR study, it is suggested that either a small spatial displacement of O^{2-} ions or a spin reorientation transition occurs at $T_{N2}=120$ K.¹¹ However, there is no indication of a spin reorientation transition in the magnetic neutron scattering [see Fig. 4(c)]. Therefore, combining with the structural analysis of the XRD data, we conclude that the drastic change in the μ^+ SR signal at T_{N2} is induced by a small spatial displacement of O^{2-} ions. Such displacement naturally leads to the change in the μ^+ sites and the number of muon-spin precession frequencies.²²

Among several theoretical work on the 1D $S=1/2$ (or 1) Heisenberg system with competing $J_1(<0)$ and $J_2(>0)$, to our knowledge, the presence of an SDW phase is predicted only when the effect of an external magnetic field is considered as⁸

$$\mathcal{H} = J_1 \sum_l s_l \cdot s_{l+1} + J_2 \sum_l s_l \cdot s_{l+2} - H \sum_l s_l^x. \quad (2)$$

Here, s_l is a $S=1/2$ operator on the site l and H is an external magnetic field, which partially polarizes spins along the x direction perpendicular to the exchange pathway of J_1 and J_2 . In the case that $J_1/J_2 \leq -1$, i.e., FM J_1 is stronger than AF J_2 , the SDW phase appears in two separated regions defined by two parameters, namely, J_1/J_2 and H/J_2 . Here, it is considered that the condition $J_1/J_2 \leq -1$ is satisfied for NaV_2O_4

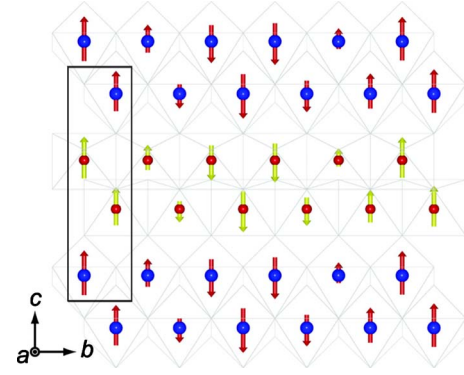


FIG. 5. (Color online) Magnetic structure of NaV_2O_4 at 20 K. Small (red) and large (blue) circles correspond to V ions at different sites (V_1 and V_2). Arrows indicate the direction and magnitude of the V moment. Na and O atoms are not shown for clarity. The average value of the ordered magnetic moment is estimated as $0.49\mu_B/V$ by integration of Eq. (1) in the whole lattices, although the effective magnetic moment (μ_{eff}) was reported as $1.99-2.70\mu_B/V$ (Ref. 4).

because $|J_1|$ is stronger than $|J_2|$ due to the large positive value Θ_p of DC- χ measurement. The SDW phase, however, never appears at $H=0$ but locates in the H range with $H/J_2 \geq 0.03$, meaning that the SDW order is only stabilized by H . This is most likely to be applicable to the insulating 1D $S=1/2$ system, such as LiCuVO_4 ,²³ but very different from the present result. In particular, although s_l^z is essential to form the SDW order in the above model, there is no x component of the spin-density wave for NaV_2O_4 by neutron measurements.

For the ground state of the V_2O_4 zigzag chain in a mixed-valence state, on the other hand, past theoretical work^{9,10} has concentrated the effort to explain the formation of a spin-gap state due to charge ordering (CO) of hollandite-type compounds, $\text{Bi}_x\text{V}_8\text{O}_{16}$ (Ref. 24) and $\text{K}_2\text{V}_8\text{O}_{16}$.²⁵ The obtained AF magnetic structure is naturally commensurate to the CO insulator lattice and, as a result, is not applicable for NaV_2O_4 . Consequently, we need a different theoretical approach on a 1D metallic system as a function of electron filling from $S=1/2$ to 1 in order to fully understand the magnetic nature of NaV_2O_4 . Consequently, it is very significant to study the change in the AF (SDW) structure with the substitution for Na by Ca in NaV_2O_4 , i.e., $\text{Na}_{1-x}\text{Ca}_x\text{V}_2\text{O}_4$, by neutron scattering, since a static magnetic order state was found by μ^+ SR in the x range between ~ 0.78 and 1.¹¹ Although the available x range is limited, such neutron experiments will provide crucial information for a novel theoretical approach and to predict the phase diagram of $\text{Na}_{1-x}\text{Ca}_x\text{V}_2\text{O}_4$. Part of such work has at present already been initiated.

In conclusion, we demonstrate the formation of an IC-SDW order in NaV_2O_4 below $T_N=140$ K by means of neutron scattering. Since the modulation period is 5.26 along the b axis (along the zigzag chain), this compound is thought to be a rare case where a 1D system exhibits a metallic AF nature. Furthermore, a precise structural analysis of the x-ray diffraction data obtained at a synchrotron-radiation source clarified the occurrence of slight distortion of the VO_6 octa-

hedron at T_{N2} . This is consistent with the appearance of the four signals in the previously obtained ZF- μ^+ SR spectrum below 120 K.¹¹

This work is based on experiments performed at the Swiss spallation neutron source SINQ and the Swiss Light Source,

SLS, Paul Scherrer Institut, Villigen, Switzerland. We are thankful to the beamline staff for valuable assistance during the experiments. This work is also supported by Grant-in-Aid for Scientific Research (B), Grant No. 19340107, MEXT, Japan. All images involving crystal structure were made with VESTA (Ref. 26).

*e1236@mosk.tytlabs.co.jp

- ¹G. E. Bacon, *Acta Crystallogr.* **14**, 823 (1961).
- ²K. Yamaji, *J. Phys. Soc. Jpn.* **51**, 2787 (1982).
- ³K. Yamaji, *J. Phys. Soc. Jpn.* **52**, 1361 (1983).
- ⁴K. Yamaura, M. Arai, A. Sato, A. B. Karki, D. P. Young, R. Movshovich, S. Okamoto, D. Mandrus, and E. Takayama-Muromachi, *Phys. Rev. Lett.* **99**, 196601 (2007).
- ⁵F. D. M. Haldane, *Phys. Rev. B* **25**, 4925 (1982).
- ⁶K. Nomura and K. Okamoto, *J. Phys. Soc. Jpn.* **62**, 1123 (1993).
- ⁷T. Hikihara, M. Kaburagi, H. Kawamura, and T. Tonegawa, *J. Phys. Soc. Jpn.* **69**, 259 (2000).
- ⁸T. Hikihara, L. Kecke, T. Momoi, and A. Furusaki, *Phys. Rev. B* **78**, 144404 (2008).
- ⁹Y. Shibata and Y. Ohta, *J. Phys. Soc. Jpn.* **71**, 513 (2002).
- ¹⁰S. Horiuchi, T. Shirakawa, and Y. Ohta, *Phys. Rev. B* **77**, 155120 (2008).
- ¹¹J. Sugiyama, Y. Ikeda, T. Goko, E. J. Ansaldo, J. H. Brewer, P. L. Russo, K. H. Chow, and H. Sakurai, *Phys. Rev. B* **78**, 224406 (2008).
- ¹²G. M. Kalvius, D. R. Noakes, and O. Hartmann, in *Handbook on the Physics and Chemistry of Rare Earths*, edited by K. A. Gschneidner, Jr., L. Eyring, and G. H. Lander (Elsevier Science B.V., Amsterdam, 2001), Vol. 32, Chap. 206, and references cited therein.
- ¹³H. Sakurai, *Phys. Rev. B* **78**, 094410 (2008).
- ¹⁴P. Fischer, G. Frey, M. Koch, M. Könnecke, V. Pomjakushin, J. Schefer, R. Thut, N. Schlumpf, R. Bürge, U. Greuter, S. Bondt, and E. Berruyer, *Physica B* **276-278**, 146 (2000).
- ¹⁵P. Fischer, L. Keller, J. Schefer, and J. Kohlbrecher, *Neutron News* **11**, 19 (2000).
- ¹⁶B. D. Patterson, R. Abela, H. Auderset, Q. Chen, F. Fauth, F. Gozzo, G. Ingold, H. Kühne, M. Lange, D. Maden, D. Meister, P. Pattison, Th. Schmidt, B. Schmitt, C. Schulze-Briese, M. Shi, M. Stambanoni, and P. R. Willmott, *Nucl. Instrum. Methods Phys. Res. A* **540**, 42 (2005).
- ¹⁷J. Rodríguez-Carvajal, *Physica B* **192**, 55 (1993).
- ¹⁸F. Izumi and T. Ikeda, *Mater. Sci. Forum* **321-324**, 198 (2000).
- ¹⁹G. Grüner, *Density Waves in Solids* (Addison-Wesley-Longmans, Reading, 1994), Chap. 4, and references cited therein.
- ²⁰L. P. Le, G. M. Luke, B. J. Sternlieb, W. D. Wu, Y. J. Uemura, J. H. Brewer, T. M. Riseman, R. V. Upasani, L. Y. Chiang, and P. M. Chaikin, *Europhys. Lett.* **15**, 547 (1991).
- ²¹U. Köbler and S. M. Dubiel, *Z. Physik B* **61**, 257 (1985).
- ²²J. Sugiyama, Y. Ikeda, P. L. Russo, H. Nozaki, K. Mukai, D. Andreica, A. Amato, M. Blangero, and C. Delmas, *Phys. Rev. B* **76**, 104412 (2007).
- ²³M. Enderle, C. Mukherjee, B. Fåk, R. K. Kremer, J.-M. Broto, H. Rosner, S.-L. Drechsler, J. Richter, J. Malek, A. Prokofiev, W. Assmus, S. Pujol, J.-L. Raggazzoni, H. Rakoto, M. Rheinstädter, and H. M. Rønnow, *Europhys. Lett.* **70**, 237 (2005).
- ²⁴H. Kato, T. Waki, M. Kato, K. Yoshimura, and K. Kosuge, *J. Phys. Soc. Jpn.* **70**, 325 (2001).
- ²⁵M. Isobe, S. Koishi, N. Kouno, J. Yamaura, T. Yamauchi, H. Ueda, H. Gotou, T. Yagi, and Y. Ueda, *J. Phys. Soc. Jpn.* **75**, 073801 (2006).
- ²⁶K. Momma and F. Izumi, *J. Appl. Crystallogr.* **41**, 653 (2008).